Uzbekistan Journal of Polymers
journal homepage: https://uzpolymerjournal.com/
ISSN (online): 2181-3256 (print) 2181-3246

CoFeNi–P/NF ELECTROCATALYST WITH ENHANCED BIFUNCTIONAL ACTIVITY FOR EFFICIENT ALKALINE WATER SPLITTING

Farhodjon Hoshimov[a,b,c], Khakimjan Butanov[a], Shavkat Mamatkulov[a] and Olim Ruzimuradov[a,d]

[a] *Institute of Materials Science, Uzbekistan Academy of Sciences, Chingiz Aytmatov 2B St., Tashkent, 100084, Uzbekistan*
[b] *National Research Institute of Renewable Energy Sources, Ministry of Energy, Chingiz Aytmatov 2B St., Tashkent, 100084, Uzbekistan*
[c.] *Institute of Fundamental and Applied Research, National Research University TIIAME, Tashkent, 100000, Uzbekistan*
[d] *Turin Polytechnic University in Tashkent, Tashkent, 100095, Uzbekistan*

ARTICLE INFO

Received: 18 November 2025
Revised: 09 February 2026
Accepted: 03 March 2026

Keywords:
bifunctional electrocatalyst, hydrogen evolution reaction, oxygen evolution reaction, water splitting, alkaline electrolysis

Corresponding author
farhod2702@gmail.com

ABSTRACT

A rationally engineered ternary phosphide electrocatalyst CoFeNi-P/NF was developed through hydrothermal growth followed by controlled vapor-phase phosphorization to address the kinetic limitations of alkaline water splitting. Phosphorization induced profound electronic modulation and surface reconstruction of the CoFeNi nanosheet framework, generating defect-rich architectures and conductive metal-phosphide networks. The incorporation of phosphorus redistributed the electronic density of Co-Fe-Ni centers, optimized hydrogen adsorption energetics (ΔG_H*), and promoted in situ formation of catalytically active (oxy)hydroxide species during OER. Structural and compositional analyses confirmed uniform elemental distribution and preservation of the interconnected nanosheet morphology. Benefiting from synergistic multimetal interaction, enhanced charge-transfer kinetics, and increased electrochemically active surface area, the CoFeNi–P/NF electrode required only 132 mV for HER and 140 mV for OER at 10 mA cm^{-2} in 1 M KOH. Notably, the catalyst exhibited outstanding durability with negligible potential decay over 50 h of continuous operation at high current density. These results demonstrate that phosphorus-engineered ternary metal phosphides supported on 3D conductive scaffolds represent a scalable and efficient strategy for developing robust noble-metal-free electrocatalysts for sustainable hydrogen production.

DOI: *10.66640/UJP-2026-5-00004*

Introduction

The global transition toward clean and carbon-neutral energy systems has reinforced the importance of developing efficient hydrogen production technologies. Hydrogen is widely recognized as a sustainable, high energy–density, and environmentally benign fuel, making it a critical component of future renewable energy infrastructures [1]. Among the various hydrogen production routes, electrochemical water splitting has gained increasing attention due to its compatibility with renewable energy sources and its ability to produce high-purity hydrogen without CO_2 emissions [2]. Despite these advantages, the overall efficiency of water splitting is

significantly hindered by the sluggish kinetics of both the hydrogen evolution reaction (HER) and the oxygen evolution reaction (OER), which require efficient electrocatalysts to reduce the required overpotential [3]. Noble-metal-based catalysts, such as Pt for HER and IrO_2/RuO_2 for OER, represent the benchmark materials due to their outstanding catalytic activities. However, their high cost, scarcity, and limited long-term stability severely restrict large-scale deployment [4,5]. Consequently, considerable research efforts have focused on developing non-noble, earth-abundant electrocatalysts with high activity and stability in alkaline environments. Transition metals such as Co, Fe, and Ni have shown tremendous promise due to their favorable redox properties, tunable electronic structures, and natural abundance [6]. Furthermore, combining these metals in ternary systems often leads to strong synergistic effects, improved electron-transfer properties, and optimized adsorption energies for reaction intermediates [7]. Recent studies have highlighted the potential of metal phosphides as high-performance electrocatalysts for both HER and OER. Phosphorus incorporation into transition metals has been shown to tune their electronic structures, increase electrical conductivity, and generate active metal–P bonds that facilitate efficient catalytic reactions [8]. Metal phosphides, including Ni_2P, CoP, FeP, and their multimetallic derivatives, have demonstrated enhanced performance in alkaline media due to favorable hydrogen adsorption energies and high corrosion resistance [9,10]. For instance, Popczun et al. demonstrated that transition-metal phosphides exhibit HER activities comparable to some noble metals [11], while Liu et al. showed that FeNiP nanosheets significantly improve HER performance through electronic coupling effects [12]. In parallel, integration of electrocatalysts onto conductive three-dimensional substrates such as nickel foam (NF) offers additional advantages, including enhanced mass transport, high mechanical stability, and rapid electron transfer [13]. NF-based electrocatalysts have shown superior performance in alkaline water splitting due to their large surface area and efficient gas release pathways [14]. The combination of multimetal synergy, phosphorus incorporation, and NF support structure is therefore a highly effective strategy for producing high-performance bifunctional catalysts. Specifically, ternary CoFeNi systems have recently attracted attention due to their enriched electronic density, favorable intermediate adsorption energies, and multi-site catalytic behavior [15]. Co contributes to improved HER kinetics, Fe enhances OER redox activity by stabilizing high-valence states, and Ni provides a conductive backbone with strong structural stability [16]. When modified with phosphorus, CoFeNi-based catalysts exhibit improved charge-transfer properties and increased catalytic turnover frequency [17]. Despite these promising developments, systematic studies combining all three elements-ternary metal synergy, phosphorus modification, and hierarchical nanosheet architectures-remain limited. Addressing this research gap, the present study investigates a phosphorized CoFeNi catalyst directly grown on NF (CoFeNi-P/NF) through a hydrothermal-phosphorization route. Comprehensive structural characterization reveals an interconnected nanosheet network with uniform Co, Fe, Ni, and P distribution. Electrochemical testing in 1 M KOH demonstrates exceptionally low overpotentials of 132 mV for HER and 140 mV for OER, outperforming many previously reported non-noble-metal catalysts. This work provides valuable insight into the design principles of ternary transition-metal phosphides supported on 3D conductive scaffolds and demonstrates their potential for high-efficiency alkaline water splitting.

Materials and Methods

2.1. Materials. Cobalt nitrate ($Co(NO_3)_2 \cdot 6H_2O$), iron nitrate ($Fe(NO_3)_3 \cdot 9H_2O$), nickel nitrate ($Ni(NO_3)_2 \cdot 6H_2O$), urea, and ammonium fluoride (NH_4F) were used in the synthesis process. Sodium hypophosphite ($NaH_2PO_2 \cdot H_2O$) was selected as the phosphorus source. Nickel foam (NF) with high porosity was employed as the substrate. All chemical reagents were of analytical grade and were used without further purification.

2.2. Synthesis of CoFeNi/NF nanocomposite

The CoFeNi nanocomposite r was synthesized via a controlled hydrothermal approach adapted from earlier multimetal hydroxide growth methods. Prior to synthesis, nickel foam (NF) substrates (2 × 3 cm^2) were cleaned through ultrasonication in ethanol for 15 minutes and then rinsed thoroughly with deionized water to remove residual surface contaminants and facilitate uniform nucleation. A homogeneous precursor solution was prepared by dissolving stoichiometric ratios of metal nitrate salts in 80 mL of deionized water: 0.5 mmol ($Co(NO_3)_2 \cdot 6H_2O$), 0.5 mmol ($Fe(NO_3)_3 \cdot 9H_2O$), and 0.5 mmol ($Ni(NO_3)_2 \cdot 6H_2O$). To assist the formation of nanosheet structures, 3 mmol NH_4F and 6 mmol urea were added, enabling slow release of OH^- ions during hydrothermal treatment. The mixture was stirred for 30 minutes until a clear pink solution was obtained. The cleaned NF substrate was immersed vertically into a 100 ml Teflon-lined stainless-steel autoclave containing the precursor solution. The autoclave was sealed and heated to 140°C for 12 hours, promoting the in situ growth of mixed-metal hydroxide nanosheets directly on NF. Following hydrothermal synthesis, the autoclave was naturally cooled to room temperature. The coated NF substrate was removed, thoroughly washed with deionized water and ethanol, and dried at 60°C for 2 hours, yielding the CoFeNi/NF precursor. The as-prepared precursor resembled typical layered hydroxide nanosheets reported for transition-metal catalysts.

2.3. Phosphorization Process to Form CoFeNi–P/NF

Phosphorization was performed using a vapor-phase thermal conversion method based on previous studies of metal phosphide formation. The dried CoFeNi/NF precursor and 1 g of NaH_2PO_2 were placed in separate ceramic boats within a quartz tube furnace to avoid direct contact. The precursor was positioned upstream, while NaH_2PO_2 was placed downstream to ensure uniform exposure to phosphine vapor (PH_3) generated during decomposition. The furnace was purged with high-purity argon for 30 minutes to remove oxygen. Subsequently, the system was heated to 300°C at a ramp rate of 2°C/min and maintained at this temperature for 2 hours. During heating, NaH_2PO_2 decomposed to release PH_3 vapor, which reacted with the precursor to form the phosphorized CoFeNi-P phase. After phosphorization, the system was allowed to cool naturally under flowing argon. The obtained material exhibited a uniform dark-gray appearance, characteristic of metal phosphides.

2.4. Structural and Morphological Characterization.

Surface morphology and nanosheet architecture were examined using a field-emission scanning electron microscope (FE-SEM, JEOL JSM-7600F). Observations revealed vertically aligned, interconnected nanosheets covering the NF substrate, providing a high surface area favorable for catalytic applications. Elemental composition and spatial distribution of Co, Fe, Ni, and P were determined via energy-dispersive X-ray spectroscopy (EDS) mapping attached to the SEM. The uniform elemental distribution indicated successful incorporation of phosphorus and homogeneous metal mixing, consistent with other ternary phosphide catalysts.

2.5. Electrochemical Measurements

Electrochemical performance was evaluated using a three-electrode configuration on a CHI 760E workstation. The CoFeNi-P/NF sample served as the working electrode. A graphite rod and Ag/AgCl (3 M KCl) electrodes were used as counter and reference electrodes, respectively. All measurements were performed in 1.0 M KOH aqueous solution at room temperature.

Linear sweep voltammetry (LSV) was conducted at a scan rate of 5 mV/s to evaluate HER and OER activities. All potentials were converted to the reversible hydrogen electrode (RHE) scale using the relation:

$$E_{RHE} = E_{Ag/AgCl} + 0.059 \times pH + 0.198 \qquad (1)$$

HER and OER overpotentials at 10 mA cm^{-2} were determined directly from the LSV curves.

Results and discussion

The surface morphologies of the CoFeNi/NF precursor and the phosphorized CoFeNi-P/NF electrocatalyst were investigated using high-resolution field-emission SEM, and the corresponding images are presented in Figure 1a–b. Distinct structural differences are observed before and after the phosphorization process, reflecting the successful conversion of the ternary metal hydroxide precursor into a metal-phosphide-based catalytic architecture. As shown in Figure 1a, the CoFeNi/NF sample exhibits a dense array of vertically aligned nanosheets uniformly grown across the entire surface of the nickel foam substrate. These nanosheets possess a sharp-edged, blade-like appearance and form a compact, highly ordered structure. The nanosheet thickness ranges from several tens of nanometers, while their lateral dimensions extend to a few hundred nanometers, giving rise to a high-aspect-ratio architecture. Such a morphology significantly increases the accessible catalytic surface area by providing numerous active edges and open channels for electrolyte diffusion. The enlarged SEM image further reveals that the nanosheets are thin, smooth, and closely interconnected, forming a continuous conductive network. This configuration facilitates rapid electron transport from the active phase to the nickel foam backbone and minimizes contact resistance during electrocatalysis. Moreover, the vertically aligned nanosheets create interconnected porous pathways that enhance ion diffusion and mass transport, both of which are critical for efficient HER and OER kinetics. The uniform growth of the nanosheet layer indicates that the hydrothermal process produced a well-defined and homogeneous multimetal hydroxide precursor. Following phosphorization, pronounced structural transformations occur, as shown in Figure 1b. Although the nanosheet architecture is preserved, the surface becomes noticeably rougher and thicker compared to the pristine precursor. The nanosheets evolve into a more corrugated and defect-rich form, displaying curved edges and a more porous texture. These changes can be attributed to the PH_3-induced vapor-phase phosphorization process, during which partial reduction, phosphorus incorporation, and surface reconstruction occur simultaneously. Higher-magnification SEM images reveal that the nanosheets in CoFeNi-P/NF are more intertwined and spaced farther apart, forming a three-dimensional open network. This structural reconstruction introduces abundant nanopores, defects, and disordered edge sites, all of which serve as favorable catalytic hotspots for both HER and OER. The increased roughness and porosity not only expand the electrochemically active surface area but also enhance the accessibility of reactant molecules to the catalytic centers. In addition, the curved nanosheet structure facilitates rapid release of generated gas bubbles, preventing accumulation on the catalyst surface during electrolysis. This effect is particularly important for OER, where trapped O_2 bubbles can hinder active sites and limit mass transport. The modified nanosheet texture therefore contributes to maintaining stable and continuous catalytic turnover. The preservation of the nanosheet network after phosphorization indicates strong mechanical integrity and firm adhesion to the nickel foam substrate. This robust interface is essential for long-term operational stability in alkaline media. Moreover, the incorporation of phosphorus into the CoFeNi lattice improves electrical conductivity and enhances charge-transfer kinetics, both of which support the improved HER and OER performance. The transformation from thin, ordered nanosheets (CoFeNi/NF) to rough, defect-rich nanosheets (CoFeNi–P/NF) is directly correlated with the superior bifunctional catalytic activity of the phosphorized sample.

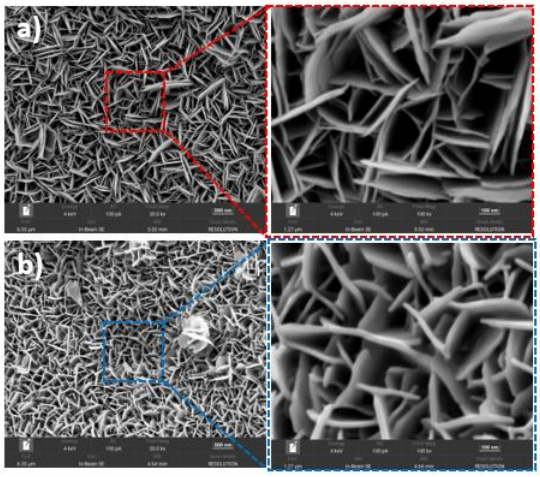

Figure 1. *SEM images of a) CoFeNi/NF, b) CoFeNi-P/NF*

The elemental composition and distribution of the phosphorized CoFeNi–P/NF electrocatalyst were further examined using energy-dispersive X-ray spectroscopy (EDS), and the corresponding results are presented in Figure 2. The EDS survey spectrum clearly shows the presence of Ni, Co, Fe, P, and O, confirming the successful formation of a multimetallic phosphide structure on the nickel foam substrate. Strong and distinct peaks corresponding to Ni arise from both the nickel foam backbone and the Ni-rich ternary alloy phase formed during hydrothermal synthesis. In addition, the well-defined phosphorus peaks demonstrate the effective incorporation of P atoms during the vapor-phase phosphorization treatment, indicating the formation of metal–phosphide bonds that are essential for enhanced HER and OER kinetics. Quantitative EDS analysis reveals the following elemental weight compositions: Ni (64.92 wt%), O (16.70 wt%), P (8.85 wt%), Fe (5.58 wt%), and Co (3.94 wt%). The relatively high Ni percentage originates from the conductive NF substrate, whereas the measurable Fe and Co contents confirm that all three transition metals are successfully integrated into the catalytic layer. Notably, the P content of 8.85 wt% indicates efficient phosphorus incorporation, which plays a crucial role in tuning the electronic environment of the catalyst and improving charge-transfer efficiency. The presence of oxygen is attributed to a thin surface oxide/hydroxide layer, a commonly observed feature in transition-metal phosphides exposed to air. Such surface species can also contribute positively to OER activity by providing additional adsorption sites for oxygen-containing intermediates. Elemental mapping images further support the homogeneous distribution of all detected elements across the nanosheet network. The Ni Kα1, Fe Kα1, and Co Kα1 maps display uniform signals, indicating that the ternary metal components are well-dispersed without noticeable aggregation or phase separation. This uniform mixing is essential for achieving synergistic interactions among Co, Fe, and Ni, which collectively enhance intrinsic catalytic activity. The P Kα1 map shows even phosphorus coverage over the entire catalyst surface, confirming complete and uniform phosphorization. Such homogeneous phosphorus distribution suggests that metal phosphide species are continuously formed throughout the nanosheets rather than localized in limited regions. The O Kα1 mapping also reveals a consistent but weaker signal, supporting the existence of a thin oxygen-rich layer that naturally forms on phosphide surfaces. This layer is known to improve wettability and facilitate fast electrolyte penetration into the catalyst. Overall, the EDS analysis demonstrates that the CoFeNi-P/NF catalyst possesses the desired multimetallic composition and uniform chemical distribution required for high-performance water-splitting electrocatalysis. The presence of uniformly dispersed Co, Fe, Ni, and P throughout the nanosheet structure ensures efficient electronic interactions, abundant active sites, and optimized catalytic pathways for both HER and OER.

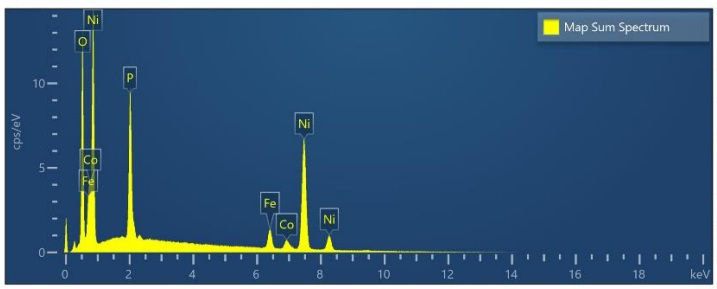

Map Sum Spectrum		
Element	Weight %	Atomic %
O	16.70	40.11
P	8.85	10.99
Fe	5.58	3.84
Co	3.94	2.57
Ni	64.92	42.49
Total	100.00	100.00

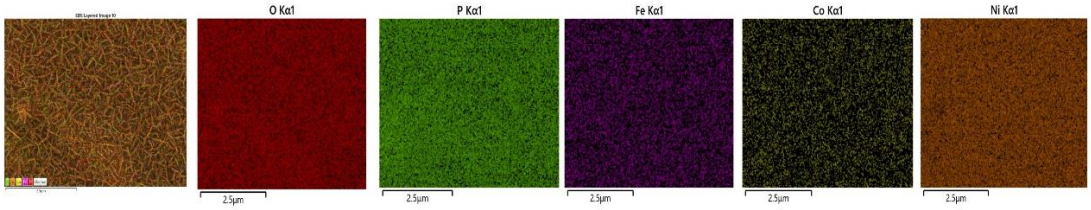

Figure 2. *EDS spectrum of CoFeNi-P/NF and EDS elemental mapping*

Electrochemical measurement for HER. Figure 3a shows the HER polarization curves of the CoFeNi/NF and CoFeNi-P/NF electrodes measured in 1.0 M KOH. The pristine CoFeNi/NF sample exhibits relatively sluggish catalytic behavior, requiring more negative potentials to reach meaningful current densities. In contrast, the CoFeNi-P/NF electrode displays a much steeper increase in cathodic current density and an earlier onset potential, indicating significantly accelerated hydrogen evolution kinetics after phosphorization. The extracted overpotential values presented in Figure 3b further highlight this enhancement. The CoFeNi/NF electrode requires 273 mV to reach 10 mA cm^{-2} and 397 mV at 50 mA cm^{-2}, demonstrating limited intrinsic HER activity. After phosphorus incorporation, the CoFeNi-P/NF catalyst achieves the same current densities at markedly lower overpotentials of only 132 mV and 258 mV, respectively. This substantial reduction clearly confirms that phosphorization improves the electronic structure of the catalyst, increases the number of active sites, and facilitates faster charge-transfer and water dissociation during HER.

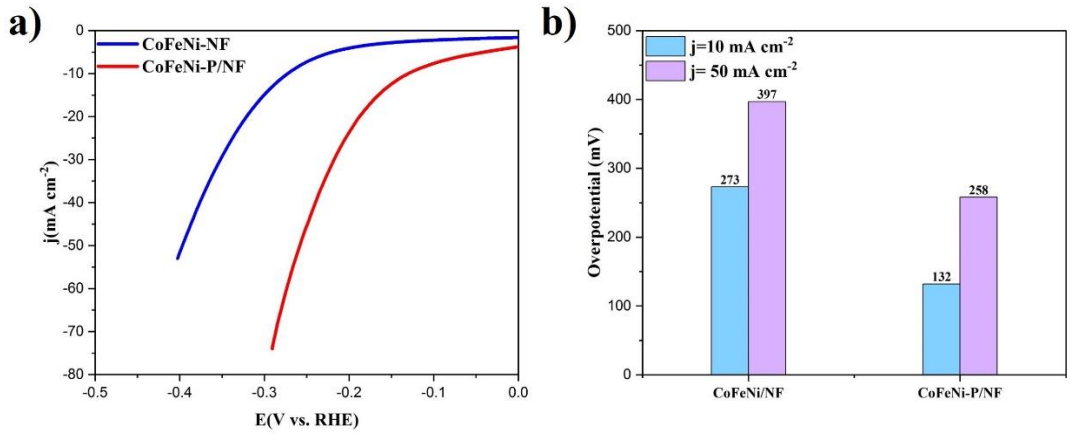

Figure 3 *HER performance under 1 M KOH: a) LSV polarization curves of asprepared catalysts for HER; b) Overpotential values of CoFeNi/NF and CoFeNi-P/NF catalysts at 10 mA cm^{-2} and 50 mA cm^{-2}*

Electrochemical measurement for OER. Figure 4a compares the OER polarization curves of the CoFeNi/NF and CoFeNi–P/NF electrodes in 1.0 M KOH. The pristine CoFeNi/NF sample shows a delayed onset potential and relatively slow increase in anodic current density, indicating sluggish oxygen evolution kinetics. In contrast, the CoFeNi–P/NF electrode displays a much earlier onset potential and considerably higher current densities across the entire potential range. This

enhanced anodic behavior clearly demonstrates that phosphorus incorporation significantly accelerates the multistep OER pathway. The overpotential values extracted from Figure 4b further confirm the improved OER performance. The CoFeNi/NF electrode requires 270 mV to achieve 10 mA cm^{-2} and 350 mV at 50 mA cm^{-2}, reflecting its limited intrinsic activity. After phosphorization, the CoFeNi–P/NF catalyst reaches the same current densities with much lower overpotentials of only 140 mV and 290 mV, respectively. This substantial reduction highlights the beneficial effects of phosphorus in modulating the electronic structure, enhancing charge-transfer efficiency, and promoting the formation and transformation of OER intermediates (OH*, O*, OOH*). Additionally, the roughened nanosheet morphology of CoFeNi-P/NF facilitates faster electrolyte penetration and more efficient oxygen bubble release, contributing to stable high-current operation.

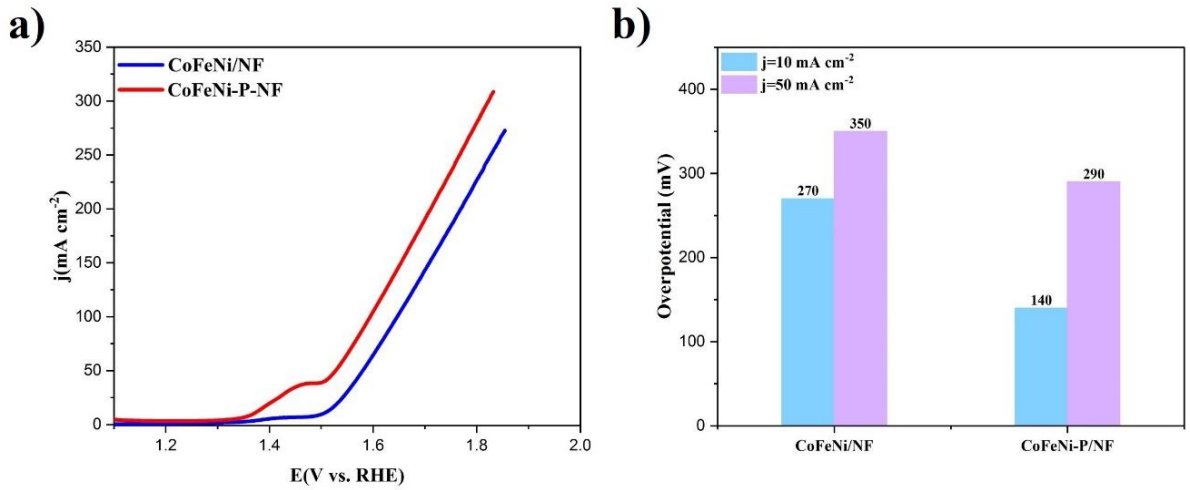

Figure 4 *OER performance under 1 M KOH: a) LSV polarization curves of asprepared catalysts for OER; b) Overpotential values of CoFeNi/NF and CoFeNi-P/NF catalysts at 10 mA* cm^{-2} *and 50 mA* cm^{-2}

The superior long-term stability of CoFeNi-P/NF, demonstrated by the negligible potential decay over 50 hours of continuous operation, further highlights the robustness of the reconstructed surface (Figure 5). The stable potential profile indicates resistance to structural degradation, dissolution, and surface oxidation. The hybrid chemical composition combining metallic phosphides with robust oxyhydroxide/phosphate layers creates a self-healing interface capable of maintaining structural integrity under prolonged alkaline electrolysis. Phosphorus not only enhances intrinsic electronic conductivity but also protects active metal centers from deactivation, preventing aggregation and surface passivation during extended cycling. Taken together, the dramatic improvement in HER activity results from a complex interplay between structural, electronic, and morphological transformation: conductive M-P networks accelerate charge transfer, defect-rich nanosheets with expanded surface area increase active-site density, favorable electronic modulation lowers ΔG_H*, enabling optimal adsorption/desorption energetics, reduced Rct facilitates fast interfacial electron transport, and hybrid phases stabilize catalytic intermediates while maintaining long-term robustness. The combination of these effects establishes CoFeNi-P/NF as a highly advanced and reliable electrocatalyst for hydrogen evolution in alkaline media, with performance characteristics that exceed those of most conventional transition-metal catalysts.

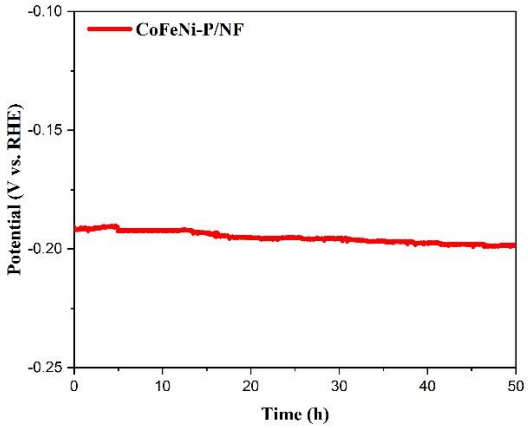

Figure 5. *HER performance under 1 M KOH: Chronoamperometry test at a curren density of 100 mA cm*$^{-2}$ *for.*

Conclusion

In this study, a design strategy integrating ternary metal synergy, phosphorus modulation, and hierarchical nanosheet engineering was successfully implemented to construct a high-performance bifunctional electrocatalyst for alkaline water splitting. The hydrothermal-phosphorization route enabled uniform formation of defect-rich CoFeNi-P nanosheets strongly anchored on a three-dimensional nickel foam scaffold, ensuring efficient electron transport and structural robustness. Phosphorus incorporation played a decisive role in tuning the electronic structure of the Co-Fe-Ni system, lowering hydrogen adsorption free energy, enhancing charge-transfer kinetics, and inducing surface reconstruction that generated abundant active sites. Under anodic conditions, the phosphide surface underwent in situ transformation into catalytically active (oxy)hydroxide species, further accelerating OER kinetics. As a result, the optimized CoFeNi-P/NF catalyst achieved low overpotentials of 132 mV for HER and 140 mV for OER at 10 mA cm^{-2} in alkaline media. Importantly, the catalyst demonstrated excellent long-term operational stability, maintaining stable performance over 50 h of continuous electrolysis at elevated current density, confirming the structural integrity of the reconstructed surface and the protective role of phosphorus-containing phases. Overall, this work provides mechanistic insight into phosphorization-induced activity enhancement and establishes ternary metal phosphides supported on conductive 3D scaffolds as promising, cost-effective, and scalable candidates for next-generation alkaline water electrolysis systems.

Acknowledgements. *The research was carried out with the financial support of Agency of Innovative Development under the Ministry of Higher Education, Science and Innovation within the framework of research project no. ALM-20230502808*

References

[1]. Yang, M.; Zhang, C.H.; Li, N.W.; Luan, D.; Yu, L.; Wen, X.; Lou, X.W. Design and Synthesis of Hollow Nanostructures for Electrochemical Water Splitting. *Adv. Sci.* 2022, *9*, 2105135.
[2]. Seh, Z.W.; Kibsgaard, J.; Dickens, C.F.; Chorkendorff, I.; Norskov, J.K.; Jaramillo, T.F. Combining theory and experiment in electrocatalysis: Insights into materials design. *Science* 2017, *355*, eaad4998.
[3]. Li, Q.; Luan, X.; Xiao, Z.; Xiao, W.; Xu, G.; Li, Z.; Wu, Z.; Wang, L. Ultrafast Microwave Synthesis of Ru-Doped MoP with Abundant P Vacancies as the Electrocatalyst for Hydrogen Generation in a Wide pH Range. *Inorg. Chem.* 2023, *62*, 9687–9694.

[4]. Wang, T.; Xie, H.; Chen, M.; D'Aloia, A.; Cho, J.; Wu, G.; Li, Q. Precious Metal-Free Approach to Hydrogen Electrocatalysis for Energy Conversion: From Mechanism Understanding to Catalyst Design. *Nano Energy* 2017, *42*, 69–89.
[5]. Zhang, H.; Chen, A.; Bi, Z.; Wang, X.; Liu, X.; Kong, Q.; Zhang, W.; Mai, L.; Hu, G. MOF-on-MOF-Derived Ultrafine Fe2PCo2P Heterostructures for High-Efficiency and Durable Anion Exchange Membrane Water Electrolyzers. *ACS Nano* 2023, *17*, 24070–24079.
[6]. Xu, Y.; Yan, Y.; He, T.; Zhan, K.; Yang, J.; Zhao, B.; Qi, K.; Xia, B.Y. Supercritical CO2-Assisted Synthesis of NiFe2O4/Vertically Aligned Carbon Nanotube Arrays Hybrid as a Bifunctional Electro catalyst for Efficient Overall Water Splitting. *Carbon* 2019, *145*, 201–208.
[7]. He, Q.; Han, L.; Tao, K. Oxygen vacancy modulated Fe-doped Co3O4 hollow nanosheet arrays for efficient oxygen evolution reaction. *Chem. Commun.* 2024, *60*, 1116.
[8]. Ding, J.; Fan, T.; Shen, K.; Li, Y. Electrochemical synthesis of amorphous metal hydroxide microarrays with rich defects from MOFs for efficient electrocatalytic water oxidation. *Appl. Catal. B-Environ.* 2021, *292*, 120174.
[9]. Shen, K.; Tang, Y.; Zhou, Q.; Zhang, Y.; Ge, W.; Shai, X.; Deng, S.; Yang, P.; Deng, S.; Wang, J. Metal-organic framework-derived S-NiFe PBA coupled with NiFe layered double hydroxides as Mott-Schottky electrocatalysts for efficient alkaline oxygen evolution reaction. *Chem. Eng. J.* 2023, *471*, 144827.
[10]. Soltani, M.; Amin, H.M.A.; Cebe, A.; Ayata, S.; Baltruschat, H. Metal-Supported Perovskite as an Efficient Bifunctional Electrocatalyst for Oxygen Reduction and Evolution: Substrate Effect. *J. Electrochem. Soc.* 2021, *168*, 034504.
[11]. Amin, H.M.A.; Zan, L.; Baltruschat, H. Boosting the bifunctional catalytic activity of Co3O4 on silver and nickel substrates for the alkaline oxygen evolution and reduction reactions. *Surf. Interfaces* 2024, *54*, 105218.
[12]. Lee, L.; Jeong, Q.; Hwang, Y.J.; An, B.; Lee, H.; Jeong, H.; Kim, G.; Park, Y.; Kim, M.; Ha, D. Basics, developments, and strategies of transition metal phosphides toward electrocatalytic water splitting: Beyond noble metal catalysts. *J. Mater. Chem. A* 2024, *12*, 28574–28594.
[13]. Hu, E.; Ning, J.; Zhao, D.; Xu, C.; Lin, Y.; Zhong, Y.; Zhang, Z.; Wang, Y.; Hu, Y. A Room-Temperature Postsynthetic Ligand
[14]. Exchange Strategy to Construct Mesoporous Fe-Doped CoP Hollow Triangle Plate Arrays for Efficient Electrocatalytic Water
[15]. Splitting. *Small* 2018, *14*, 1704233.
[16]. Wang, L.; He, W.; Yin, D.; Xie, Y.; Zhang, H.; Ma, Q.; Yu, W.; Yang, Y.; Dong, X. Achieving efficient urea electrolysis by spatial
[17]. confinement effect and heterostructure. *Chem. Eng. J.* 2023, *463*, 142254.
[18]. Wang, Y.; Dong, Q.; Du, X.; Zhang, X. Mn-doped nickel-copper phosphides as oxygen evolution reaction electrocatalyst in alkaline
[19]. seawater solution. *Int. J. Hydrogen Energ.* 2024, *69*, 895–904.
[20]. Arunkumar, P.; Gayathri, S.; Han, J.H. Impact of an Incompatible Atomic Nickel-Incorporated Metal-Organic Framework on
[21]. Phase Evolution and Electrocatalytic Activity of Ni-Doped Cobalt Phosphide for the Hydrogen Evolution Reaction. *ACS Appl.*
[22]. *Energy Mater.* 2022, *5*, 2975–2992.
[23]. Huang, J.; Li, J.; Liu, R.; Wang, R.; Luo, Z.; Zou, P.; Zhu, X.; Liao, Q. Oxygen evolution reaction enhancement enabled by a Ni-doped cobalt-based phosphate electrode with hierarchical pore structures. *Int. J. Hydrogen Energ.* 2024, *64*, 724–732. [CrossRef].